



HAL
open science

1/f Tunnel Current Noise through Si-bound Alkyl Monolayers

Nicolas Clement, Stephane Pleutin, Oliver Seitz, Stephane Lenfant,
Dominique Vuillaume

► **To cite this version:**

Nicolas Clement, Stephane Pleutin, Oliver Seitz, Stephane Lenfant, Dominique Vuillaume. 1/f Tunnel Current Noise through Si-bound Alkyl Monolayers. 2007. hal-00125398v2

HAL Id: hal-00125398

<https://hal.science/hal-00125398v2>

Preprint submitted on 10 May 2007 (v2), last revised 29 Sep 2007 (v3)

HAL is a multi-disciplinary open access archive for the deposit and dissemination of scientific research documents, whether they are published or not. The documents may come from teaching and research institutions in France or abroad, or from public or private research centers.

L'archive ouverte pluridisciplinaire **HAL**, est destinée au dépôt et à la diffusion de documents scientifiques de niveau recherche, publiés ou non, émanant des établissements d'enseignement et de recherche français ou étrangers, des laboratoires publics ou privés.

$1/f^\gamma$ Tunnel Current Noise through Si-bound Alkyl Monolayers

Nicolas Clément¹, Stéphane Pleutin¹, Oliver Seitz², Stéphane Lenfant¹ and Dominique Vuillaume^{1,a}

¹ "Molecular Nanostructures and Devices" group, Institute for Electronics, Microelectronics and Nanotechnology, CNRS, BP60069, Avenue Poincaré, F-59652 cedex, Villeneuve d'Ascq, France

² Department of Materials and Interfaces, Weizmann Institute of Science, Rehovot, Israel

Abstract

We report low frequency tunnel current noise characteristics of an organic monolayer tunnel junction. The measured devices, n-Si/alkyl chain (C₁₈H₃₇)/Al junctions, exhibit a clear $1/f^\gamma$ power spectrum noise with $1 < \gamma < 1.2$. We observe a slight bias-dependent background of the normalized current noise power spectrum (S_I/I^2). However, a local increase is also observed over a certain bias range, mainly if $V > 0.4$ V, with an amplitude varying from device to device. We attribute this effect to an energy-dependent trap-induced tunnel current. We find that the background noise, S_I , scales with $(\partial I / \partial V)^2$. A model is proposed showing qualitative agreements with our experimental data.

^a Corresponding author : dominique.vuillaume@iemn.univ-lille1.fr

Molecular electronics is a challenging area of research in physics and chemistry. Electronic transport in molecular junctions and devices has been widely studied from a static (dc) point of view.^{1,2} More recently electron – molecular vibration interactions were investigated by inelastic electron tunneling spectroscopy.³ In terms of the dynamics of a system, fluctuations and noise are ubiquitous physical phenomena. Noise is often composed of $1/f$ noise at low frequency and shot noise at high frequency. Although some theories about shot noise in molecular systems were proposed,⁴ it is only recently that it was measured, in the case of a single D₂ molecule.⁵ Low frequency $1/f$ noise was studied in carbon nanotube transistors,⁶ but, up to now, no study of the low frequency current noise in molecular junctions (e.g., electrode/short molecules/electrode) has been reported. Low frequency noise measurements in electronic devices usually can be interpreted in terms of defects and transport mechanisms.⁷ While it is obvious that $1/f$ noise will be present in molecular monolayers as in almost any system, only a detailed study can lead to new insights in the transport mechanisms, defect characterization and coupling of molecules with electrodes.

We report here the first observation and detailed study of the $1/f$ power spectrum of current noise through organic molecular junctions. n-Si/C₁₈H₃₇/Al junctions were chosen for these experiments because of their very high quality, which allows reproducible and reliable measurements.⁸ The noise current power spectra (S_I) are measured for different biases. Superimposed on the background noise, we observe noise bumps over a certain bias range and propose a model that includes trap-induced tunnel current, which satisfactorily describes the noise behaviour in our tunnel molecular junctions.

Si-C linked alkyl monolayers were formed on Si(111) substrates (0.05-0.2 $\Omega\cdot\text{cm}$) by thermally induced hydrosilylation of alkenes with Si:H, as detailed elsewhere.^{8,9} 50 nm thick aluminium contact pads with different surface areas between 9×10^{-4} cm^2 and 4×10^{-2} cm^2 were deposited at 3 $\text{\AA}/\text{s}$ on top of the alkyl chains. The studied junction, Si-n/ $\text{C}_{18}\text{H}_{37}$ /Al, is shown in Fig.1 (inset). Figure 1 shows typical current density – voltage (J - V) curves. We measured 13 devices with different pad areas. The maximum deviation of the current density between the devices is not more than half an order of magnitude. It is interesting to notice that although devices A and C have different contact pad areas (see figure caption), their J - V curves almost overlap. This confirms the high quality of the monolayer.⁹ The inset of Fig. 1 shows a linear behaviour around zero bias. For most of the measured devices, the J - V curves diverge from that of device C at $V > 0.4$ V, with an increase of current that can reach an order of magnitude at 1 V (device B). Taking into account the difference of work functions between n-Si and Al, considering the level of doping in the Si substrate (resistivity ~ 0.1 $\Omega\cdot\text{cm}$), there will be an accumulation layer in the Si at $V > -0.1$ V.¹⁰ From capacitance-voltage (C - V) and conductance-frequency (G - f) measurements (not shown here), we confirmed this threshold value (± 0.1 V). As a consequence, for positive bias, we can neglect any large band bending in Si (no significant voltage drop in Si). The J - V characteristics are then calculated with the Tsu-Esaki formula¹¹ that can be recovered from the tunnelling Hamiltonian.¹² Assuming the monolayer to be in between two reservoirs of free quasi-electrons and the system to be invariant with respect to translation in the transverse directions (parallel to the electrode plates) we get

$$J(V) = \frac{emk_B\theta}{2\pi^2\hbar^3} \int_0^{+\infty} dE T(E) \ln\left(\frac{1 + e^{\beta(\mu-E)}}{1 + e^{\beta(\mu-eV-E)}}\right) \quad (1)$$

where e is the electron charge, m the effective mass of the charge carriers within the barrier, k_B the Boltzmann constant, \hbar the reduced Planck constant, μ the Fermi level and $\beta = 1/k_B\theta$ (θ the temperature in K). $T(E)$ is the transfer coefficient for quasi-electrons flowing through the tunnel barrier with longitudinal energy E . The total energy, E_T , of quasi-electrons is decomposed into a longitudinal and a transverse component, $E_T = E + E_t$; E_t was integrated out in Eq. (1). The transfer coefficient is calculated for a given barrier height, Φ , and thickness, d , and shows two distinct parts: $T(E) = T_1(E) + T_2(E)$. $T_1(E)$ is the main contribution to $T(E)$ that describes transmission through a defect-free barrier. $T_2(E)$ contains perturbative corrections due to assisted tunnelling mechanisms induced by impurities located at or near the interfaces. The density of defects is assumed to be sufficiently low to consider the defects as independent from each other, each impurity at position \vec{r}_i interacting with the incoming electrons via a strongly localized potential at

energy $U_i, U_i\delta(\vec{r} - \vec{r}_i)$, The value of U_i is random. We write $T_2(E) = \sum_{i=1}^{N_{imp}} T_2(E, U_i)$, with

N_{imp} being the number of impurities and $T_2(E, U_i)$ the part of the transmission coefficient due to the impurity i . The two contributions of $T(E)$ are then calculated following the method of Appelbaum and Brinkman.¹³ Using Eq. (1), good agreements with experiments are obtained. As examples, the theoretical J - V characteristic for device C and B are shown in Fig. 1. The best fits are obtained with $\Phi = 4.7$ eV, $m = 0.614 m_e$ (m_e is the electron mass), 10^{10} traps/cm² uniformly distributed in energy for device C and additional 10^{13} traps/cm² for device B distributed according to a Gaussian peaked at 3 eV. The transfer coefficients $T_2(E, U_i)$ show pronounced quasi-resonances at energies depending

on U_i that explain the important increase of current. The thickness is kept fixed, $d = 2$ nm (measured by ellipsometry⁸).

We now demonstrate that the difference observed in the J - V curves are well correlated with specific behaviours observed in the low frequency noise. Figure 2 shows the low frequency current noise power spectrum S_I for different bias voltages from 0.02 V to 0.9 V. All curves are almost parallel and follow a perfect $1/f^\gamma$ law with $\gamma = 1$ at low voltages, increasing up to 1.2 at 1 V. We could not observe the shot noise because the high gains necessary for the amplification of the low currents induce a cut-off frequency of our current preamplifier lower than the frequency of the $1/f$ – shot noise transition. At high currents, $1/f^\gamma$ noise was observed up to 10 kHz.

In most systems, the low frequency $1/f$ current noise usually scales as I^2 , where I is the dc tunnel current,¹⁴ as proposed for example by the standard phenomenological equation due to Hooge¹⁵ $S_I = \alpha_H I^2 / N_c f$. N_c is the number of free carriers in the sample and α_H is a dimensionless constant frequently found to be 2×10^{-3} . This expression was used with relative success for simple systems such as homogeneous bulk metals^{14,15} and more recently also for carbon nanotubes.⁶ Similar relations were also derived for $1/f$ noise in variable range hopping conduction.¹⁶ In Fig. 3.a we present the normalized current noise power spectrum (S_I/I^2) at 10 Hz (it is customary to compare noise spectra at 10 Hz) as a function of the bias V for devices B and C. Device C has a basic characteristic with the points following the dashed line asymptote. Therefore, we use it as a reference for comparison with other devices. One can note that basically S_I/I^2 decreases with $|V|$. Given this unusual current dependence on the noise, one can not express the noise using Hooge's law. Although the microscopic mechanisms associated with conductance

fluctuations in general have yet to be identified, it is believed that for many materials, the underlying mechanism involves the trapping of charge carriers in localized states.¹⁷ For most samples, in addition to the background normalized noise, we observe a local (Gaussian with V) increase of noise at $V > 0.4$ V. The amplitude of the local increase varies from device to device (shown here for devices B and C). This local increase of noise is correlated with the increase of current seen already in the J - V curves. The J - V characteristics of device B diverge from those of device C at $V > 0.4$ V and this is consistent with the local increase of noise observed in Fig. 3. Thus, the observed excess noise bump is likely to be attributed to the Gaussian distribution of traps centred at 3 eV responsible for the current increase. We will see that this is indeed the case. The nature and origin of these traps is however not known. We can hypothesis that the low density of traps uniformly distributed in energy may be due to Si-alkyl interface defects or traps in the monolayer, while the high density, peaked in energy, may be due to metal-induced gap states (MIGS)¹⁸ or residual aluminum oxide at the metal-alkyl interface. More $1/f$ noise experiments on samples with various physical and chemical natures of the interfaces are in progress.

To model the tunnel current noise in the monolayers, we assume that some of the impurities may trap charge carriers. Since we do not know the microscopic details of the trapping mechanisms and the exact nature of these defects, we introduce a qualitative description that associates to each of them an effective Two-Level Tunnelling Systems (TLTS) characterized by an asymmetric double well potential with the two minima separated in energy by ε_i . We denote as Δ_i the term allowing tunneling from one well to the other, and get, after diagonalization, two levels that are separated in energy

by $E_i = \sqrt{\varepsilon_i^2 + \Delta_i^2}$. Since we are interested in low frequency noise, we focus on defects with very long trapping times i.e. defects for which $\Delta_i \ll \varepsilon_i$. The lower state (with energy E_i^-) corresponds to an empty trap, the upper state (with energy E_i^+) to a charged one. The relaxation rate from the upper to the lower state should be determined by the coupling with the phonons and/or with the quasi-electrons giving $\tau^{-1} \propto E_i \Delta_i^2 \coth \frac{E_i}{2k_B\theta}$ and $\tau^{-1} \propto \frac{\Delta_i^2}{\hbar E_i} \coth \frac{E_i}{2k_B\theta}$, respectively. In all cases, the time scale of the relaxation, τ , is very long compared to the duration of a scattering event. This allows us to consider the TLTS with a definite value at any instant of time. We then consider the following spectral density of current for each TLTS¹⁹

$$S_i^i(f) = \overline{(I_- - I_+)^2} \frac{\tau}{1 + \varpi^2 \tau^2} \text{Cosh}^{-2} \frac{E_i}{2k_B\theta} \quad (2)$$

where $\varpi = 2\pi f$ and $I_{-(+)}$ is the tunnel current for the empty (charged) impurity state. In this equation the average of $(I_- - I_+)$ over the TLTSs, having similar ε_i and Δ_i is taken. The difference between the two levels of current has two different origins. The first one is the change in energy of the impurity level that directly affects $T_2(E)$. The second one is the change in the charge density at the interfaces of the molecular junction induced by the trapped quasi-electron that produces a shift in the applied bias, δV . We write

$$I_+(V) \cong I_-(V + \delta V) + A \frac{emk_B\theta}{2\pi^2\hbar^3} \int_0^{+\infty} dE \left. \frac{\partial T_2(E, U_i)}{\partial U_i} \right|_{E_i^-} E_i \ln \left(\frac{1 + e^{\beta(\mu-E)}}{1 + e^{\beta(\mu-eV-\delta V-E)}} \right) \quad (3)$$

where A is the junction (metal electrode) area. The first term in the right hand side is due to the fluctuating applied bias, the second to the change in impurity energy. Since $T_2(E)$ is

already a perturbation, the second contribution is in general negligible but becomes important to explain the excess noise. We focus first on the background noise and therefore we keep only the first term of Eq. (3). Moreover, we assume for simplicity that all the charged impurities give the same shift of applied bias and take $\delta V = e/C_{TJ}A$, where C_{TJ} is the capacitance of the tunnel junction per unit surface, which is observed to be almost constant for positive bias. By using the usual approximation regarding the distribution in relaxation times, τ , and energies, E_i ,¹⁹ we finally get

$$S_I \propto E^* \frac{1}{A} N_{imp}^* \left(\frac{\partial I}{\partial V} \Big|_- \right)^2 \frac{e^2}{C_{TJ}^2} \frac{1}{f}. \quad (4)$$

We assume, in particular, the distribution function of ε_i and Δ_i , $P(\varepsilon_i, \Delta_i)$, to be uniform to get the $1/f$ dependence. In this last expression, the derivative of the current is evaluated for the lower impurity state, N_{imp}^* is the impurity density per unit energy and surface area. $E^* = E_{\max}$, the maximum of E_i , if $E_{\max} \ll k_B\theta$ and $E^* = k_B\theta$ if $E_{\max} \gg k_B\theta$. It is important to stress that N_{imp}^* cannot be determined accurately from the last equation because of lack of information concerning the microscopic nature of the traps.

We confirm this predicted dependence of S_I on $(\partial I / \partial V)^2$. In Fig.4, S_I vs. $(\partial I / \partial V)$ is plotted on a log-log scale for device C. We clearly identify a slope 2. At the same time (see inset), it is very interesting to notice that $S_I - I$ also follows a power law with a slope of 1.7 and not 2 as usually assumed. The value $1.7 < 2$ explains why the normalized noise S_I/I^2 decreases with V (Fig. 3). The appropriate normalization factor to obtain flat background noise is $S_I/I^{1.7}$. These two features imply that $(\partial I / \partial V)^2$ scales with $I^{1.7}$ which has been experimentally verified from the $I-V$ curves (not shown). The

normalized noise of the devices B and C is estimated in Fig. 3.b, using Eq. (4). Qualitative agreements with the experimental data are obtained. With few defects uniformly distributed (device C), S_I/I^2 follows at low voltages the dashed line asymptote. With additional defects with a Gaussian distribution (device B), a local increase is found at the correct position but with much too small amplitude. To get a better estimate it is essential to take into account the second term of Eq. (3). Results are shown in Fig. 3.b taking $E^* = 5e\delta V$. The quasi resonances of $T_2(E)$ are at the origin of the local increase: the Gaussian distribution selects defects for which $T_2(E, U_i)$ shows quasi resonance in the appropriate range of energy. Moreover, these traps may be associated to a non-uniform contribution to the distribution function $P(\varepsilon_i, A_i)$ that would break the $1/f$ dependence of S_I above certain bias. This is indeed what is observed in Fig. 2, with γ changing from 1 to 1.2.

In summary, we have reported the first low frequency ($1/f^\gamma$) current noise in molecular junctions. We have correlated the small dispersion observed in dc J - V characteristics and the local increase of normalized noise at certain biases (mainly at $V > 0.4$ V). A theoretical model qualitatively explains this effect as due to the presence of an energy-localized distribution of traps. The model predicts that the power spectrum of the background current noise is proportional to $(\partial I / \partial V)^2$ as observed in our experiments.²⁰ We also show that the power spectrum of the current noise should be normalized as $S_I/I^{1.7}$. Finally, the low density of traps

We are indebted to David Cahen for his support and great interest in this work and very valuable discussions in several occasions. N.C. and S.P. thank the "ACI

nanosciences" program and IRCICA for post-doc grants, respectively. We thank Hiroshi Inokawa, Frederic Martinez for helpful comments.

Figure Captions:

Fig.1: Experimental J - V curves at room temperature for n-Si/C₁₈H₃₇/Al junctions. The contact areas are 0.36 mm² for device A and 1 mm² for devices B and C. The voltage V is applied to the aluminium pad and the Si is grounded, using a semiconductor signal analyzer Agilent 4155C. Each curve was acquired with a trace-retrace protocol and repeated 3 times with different delay times between each measurement (voltage step $\Delta V=1$ mV) in order to check a possible hysteresis effect and confirm that no transient affects the dc current characteristics. Theoretical J - V curves are also shown for devices B and C. The inset shows the conductance per unit area ($\delta J/\delta V$) around zero bias for the three samples.

Fig.2: Low frequency ($1/f^\gamma$) power spectrum current noise for device C. Although we measured all spectra of the sequence $|V|=[0.02; 0.05; 0.1; 0.15; 0.2; 0.25; 0.3; 0.35; 0.4; 0.45; 0.5; 0.6; 0.7; 0.8; 0.9; 1 \text{ V}]$, we selected for this figure only spectra with $V > 0$ V and a spacing of 0.2 V for clearer presentation. γ varies from 1 at low voltages to 1.2 at 1 V. For noise measurements, the experimental setup was composed of a low noise current-voltage preamplifier (Stanford SR570), powered by batteries, and a spectrum analyser (Agilent 35670A). All the measurements were performed under controlled atmosphere (N₂) at room temperature.

Fig.3: (A) Normalized power spectrum current noise S_I/I^2 as a function of bias V for devices B and C. The curve for device C follows asymptotes (black dashed lines) which are used as a reference for other devices. A local increase of noise over the asymptotes

with a Gaussian shape (red lines) is shown. **(B)** Theoretical estimates are shown for $V > 0$, based on Eq. (4) with a uniform defect distribution (solid green line), with adding a Gaussian energy-localized distribution of defects (dot blue line), and keeping the two terms of Eq. (3) with $E^* = 5e\delta V$ (blue solid line). An ad-hoc multiplicative factor has been applied to the theoretical results.

Fig.4: $S_I - (\partial I / \partial V)$ curve for device C on a log-log scale. The dashed line represents the slope of 2. In the inset, the $S_I - I$ curve is also presented on a log-log scale with a slope of 1.7.

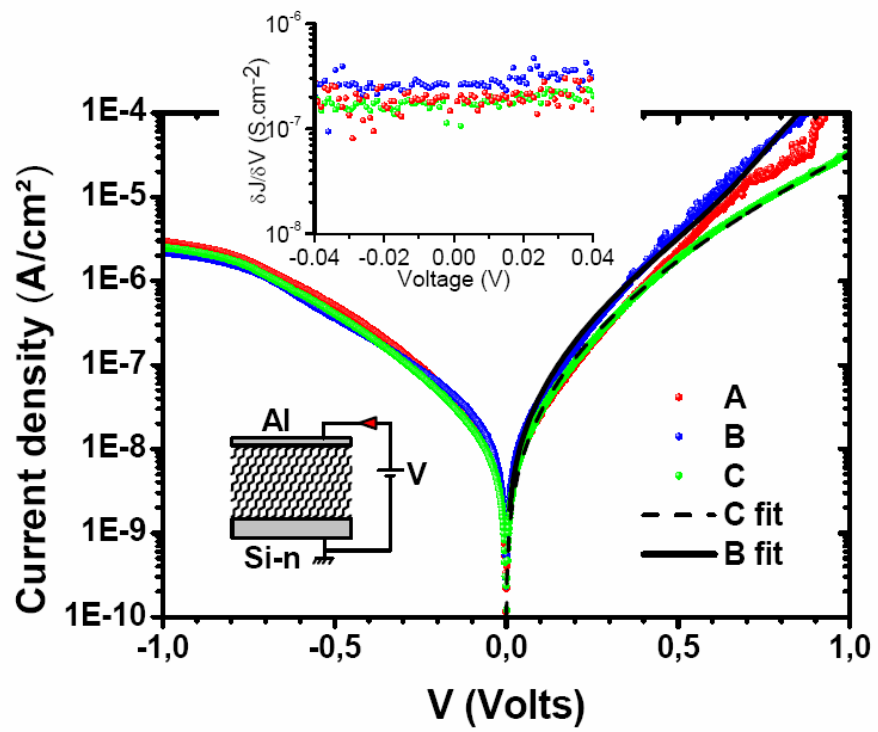


Fig.1

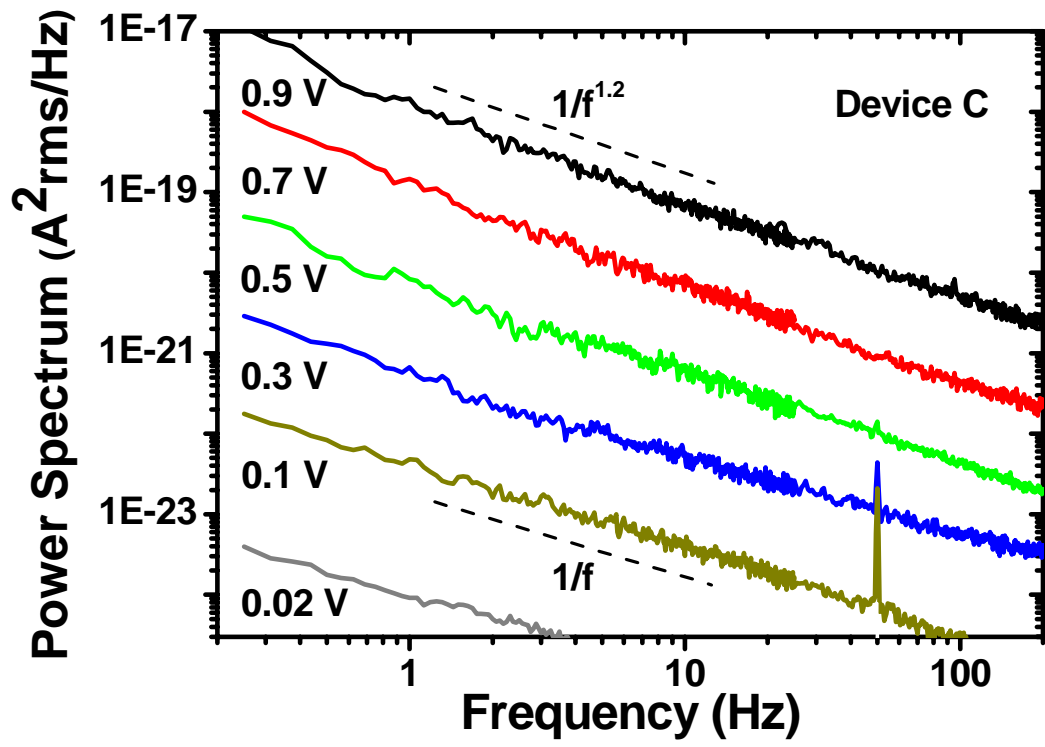


Fig.2

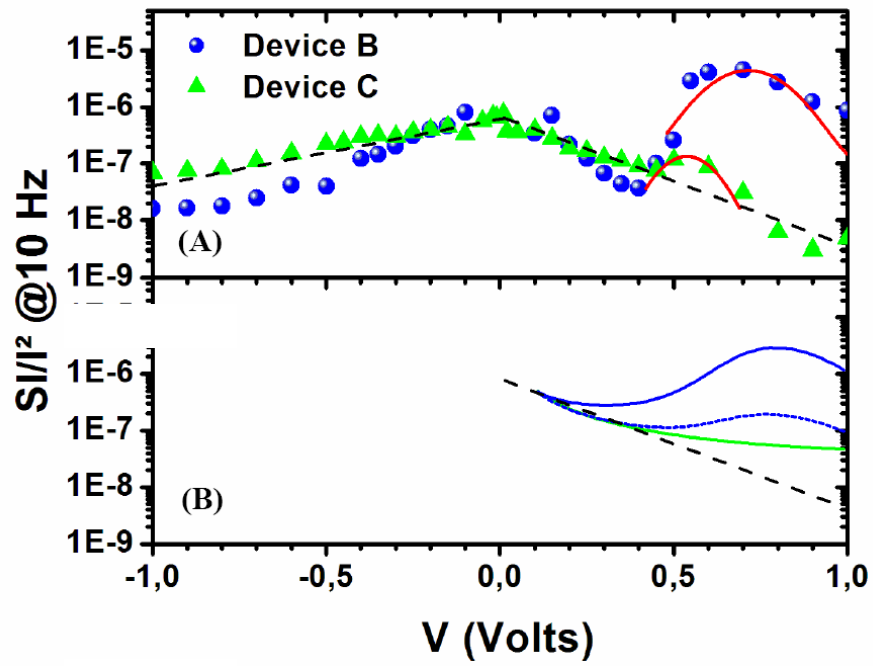


Fig.3

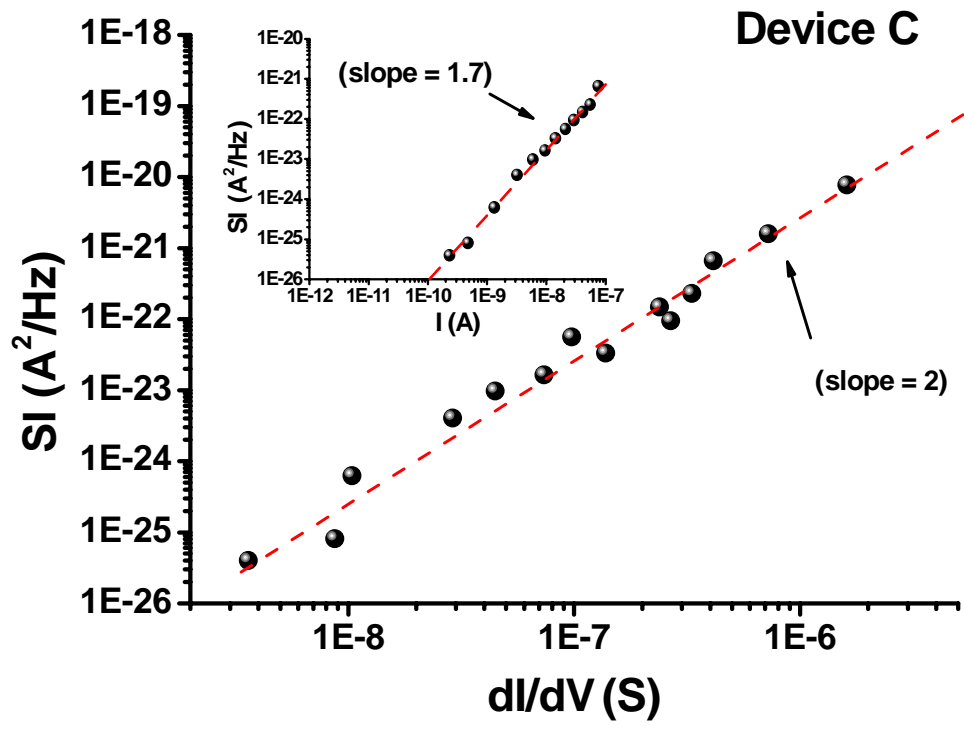


Fig.4

-
- ¹ A. Nitzan and M. A. Ratner, *Science* **300**, 1387 (2003).
- ² A. Salomon, D. Cahen, S. Lindsay, J. Tomfohr, V. B. Engelkes, and C. D. Frisbie, *Adv. Mater.* **25**, 1881 (2003).
- ³ W. Wang, T. Lee, I. Krestchmar, et al., *Nano Lett.* **4**, 643 (2004); J. G. Kushmerick, J. Lazorcik, C. H. Patterson, et al., *Nano Lett.* **4**, 643 (2004); A. Troisi and M. A. Ratner, *Phys. Rev. B* **72**, 033408 (2005); D. K. Aswal, C. Petit, G. Salace, et al., *Phys. Stat. Sol. (a)* **203**, 1464 (2006); C. Petit, G. Salace, S. Lenfant, et al., *Microelectronic Engineering* **80**, 398 (2005).
- ⁴ M. Galperin, A. Nitzan, and M. A. Ratner, *Phys. Rev. B* **74**, 075326 (2003); A. Thielmann, M. H. Hettler, J. König, and G. Schön, *Phys. Rev. B* **68**, 115105 (2003); A. Thielmann, M. H. Hettler, J. König, and G. Schön, *Phys. Rev. Lett.* **95**, 146806 (2005); R. Guyon, T. Jonckheere, V. Mujica, A. Crépieux, and T. Martin, *J. Chem. Phys.* **122**, 144703 (2005).
- ⁵ D. Djukic and J.M. van Ruitenbeek, *Nano Lett.* **6**, 789 (2006).
- ⁶ P. G. Collins, M. S. Fuhrer, and A. Zettl, *Appl. Phys. Lett.* **76**, 894 (2000); Y.-M. Lin, J. Appenzeller, J. Knoch, Z. Chen, and P. Avouris, *Nano Lett.* **6**, 930 (2006).
- ⁷ M. J. Kirton and M. J. Uren, *Adv. in Physics*, **38**, 367 (1989).
- ⁸ A. Salomon, T. Boecking, C. K. Chan, F. Amy, O. Girshevitz, D. Cahen, and A. Kahn, *Phys. Rev. Lett.* **95**, 266807 (2005).
- ⁹ O. Seitz, T. Böcking, A. Salomon, J. J. Gooding, and D. Cahen, *Langmuir* **22**, 6915 (2006).

-
- ¹⁰ S. M. Sze, *Physics of Semiconductor Devices* (Wiley, New York, 1981).
- ¹¹ R. Tsu and L. Esaki, *Appl. Phys. Lett.* **22**, 562 (1973).
- ¹² G. D. Mahan, *Many-Particle Physics*, 3rd Ed. (Plenum, New York, 2000).
- ¹³ J. A. Appelbaum and W. F. Brinkman, *Phys. Rev.* **B 2**, 907 (1970).
- ¹⁴ P. Dutta and P. M. Horn, *Rev. Mod. Phys.* **53**, 497 (1981); M. B. Weissman, *Rev. Mod. Phys.* **60**, 537 (1988).
- ¹⁵ F. N. Hooge, *Physica (Amsterdam)* 83 B, 14 (1976); F. N. Hooge, T. G. M. Kleinpenning, and L. K. J. Vandamme, *Rep. Prog. Phys.* **44**, 479 (1981).
- ¹⁶ B. I. Shklovskii, *Phys. Rev.* **B 67**, 045201 (2003); A. L. Burin, B. I. Shklovskii, V. I. Kozub, Y. M. Galperin, and V. Vinokur, *Phys. Rev.* **B 74**, 075205 (2006).
- ¹⁷ S. Machlup, *J. Appl. Phys.* **25**, 341 (1954); C. T. Rogers and R. A. Buhrman, *Phys. Rev. Lett.* **53**, 1272 (1984).
- ¹⁸ M. Kiguchi et al., *Phys. Rev. B* **72**, 075446 (2005); H. Vasquez et al., *Europhys. Lett.* **65**, 802 (2004).
- ¹⁹ S. M. Kogan, *Electronic noise and fluctuations in solids*, (Cambridge University Press, 1996).
- ²⁰ Note that a similar behavior have been some time observed in SiO₂ tunnel devices, see: G. B. Alers, K. S. Krisch, D. Monroe, B. E. Weir, and A. M. Chang, *Appl. Phys. Lett.* **69**, 2885 (1996); F. Martinez, S. Soliveres, C. Leyris, and M. Valenza, *IEEE ICMTS Proceedings*, 193 (2006).